HIGH TECHNOLOGY LETTERS | Vol. 20 No. 3 | Sep. 2014 | pp. 230 ~ 236

doi:10.3772/j.issn.1006-6748.2014.03.002

An ISS-OFDM based adaptive filtering mechanism for interference suppression in wireless multi-hop communication network①

Qin Danyang (秦丹阳)②*, Ma Lin**, Xu Renheng***, Ding Qun*

(* Key Laboratory of Electronics Engineering, Heilongjiang University, Harbin 150080, P. R. China)

(** Communication Research Center, Harbin Institute of Technology, Harbin 150080, P. R. China)

(*** Harbin Research Institute of Electrical Instruments, Harbin 150028, P. R. China)

Abstract

The negative impact on communication performance in wireless multi-hop communication network caused by limited bandwidth, high bit error rate (BER), fading, noise and interference is alleviated by an adaptive filtering game based on frequency subbands selection and predetermined threshold. Such threshold is being obtained in Gaussian and multipath fading channel according to the frequency-matching principle and BER performance. The dynamic selection of subbands will obtain high use efficiency without the help of frequency hopping, and propound a new thought to improve band limited communication for wireless multi-hop communication network. The effectiveness of the adaptive filtering method has been verified by interleaving spread spectrum orthogonal frequency division multiplexing (ISS-OFDM) in different interference conditions, and the simulating results based on network simulator 2 (NS2) indicate that system BER can be improved greatly.

Key words: multi-hop communication, adaptive filtering, interleaving spread spectrum orthogonal frequency division multiplexing (ISS-OFDM), interference suppression

0 Introduction

Wireless multi-hop network, with the typical form of ad hoc network and wireless sensor network, is usually a kind of self-organized distributed network, without any central entity. Since no infrastructure or centralized control unit exists, the nodes can move randomly and need to observer or communicate hop by hop. So each node in such kind of network is the terminal as well as a router[1,2]. As an important component of the modern communication system, the wireless spectrum sharing makes this kind of network suffer a lower transmission bandwidth[3]. Moreover, the characteristic of the mobile nodes or sensors contending for the channel makes the real bandwidth occupation far smaller than the maximum transmission rate provided by the physical layer. It is the arbitrarily moving characteristic of the nodes that will induce the dynamical changing of the network topology, which will worsen the effect on system performance of limited bandwidth, link capacity flapping, high bit error rate and so on. With the addition of factors like multiple access, fading, noise and interference, throughput of wireless mobile multi-hop network is always much lower than the maximum wireless transmission rate. Therefore, a kind of self-adaptive filtering technique is always adopted to alleviate the impact on the deep fading of subband signal in subcarrier groups so as to realize wireless channel interference suppression and to improve the communication performance[4-6]. The redistribution of transmitting signal power out of the frequency subband, however, will be sure to increase the energy of the residue subband signal, and will extend the interference effect, which has seldom been considered in the existed researches. An ISS-OFDM (interleaving spread spectrum orthogonal frequency division multiplexing) signal transmitting based adaptive filtering mechanism has been put forward in this paper for wireless multi-hop communication, which will enhance the selectivity of multi-frequency subbands transmission by the adaptive interference determined threshold in Gaussian and multi-fading channel. This novel mechanism will bring light on an adaptive data transmission

① Supported by the National Nature Science Foundation of China (No. 61302074), the Specialized Research Fund for the Doctoral Program of Higher Education (No. 20122301120004), the Natural Science Foundation of Heilongjiang Province (No. QC2013C061) and Research Foundation of Education Bureau of Heilongjiang Province (No. 12531480).

② To whom correspondence should be addressed. E-mail: qindanyang@hlju.edu.cn.

Received on May 29, 2013

technology of dynamic subband without any help of frequency hopping.

The rest of this paper is organized as follows. Section 1 reviews the previous work, as well as the generating and receiving process of ISS-OFDM. The receiver adaptive filtering approach is presented in Section 2, and Section 3 addresses the setting of determined threshold for Gaussian channel and the multiple fading channel respectively. The system performance with relative analysis is provided in Section 4. Finally, a conclusion is drawn in Section 5.

1 Motivation and description

The generating and receiving process of ISS-OFDM is shown in Fig. 1, the system model of which consists of transmitter, receiver and wireless channel.

The transmitter includes a serial-parallel converter (SPC), a complex exponential spread-spectrum modulator, a interleaving adding cyclic prefix (ACP) module and a sending filter[7,8], where the complex exponential spread-spectrum modulator and interleaver will co-generate multiple subband interleaving spread-spectrum OFDM signals[9,10]. The receiver includes an adaptive filter, adding-removing cyclic prefix (ARCP) module, parallel fast Fourier transform (FFT) demodulator, frequency-domain equalizer and maximal ratio combining (MRC) which has been adopted to filter out the useful part in multiple subband signals to restore the original information.

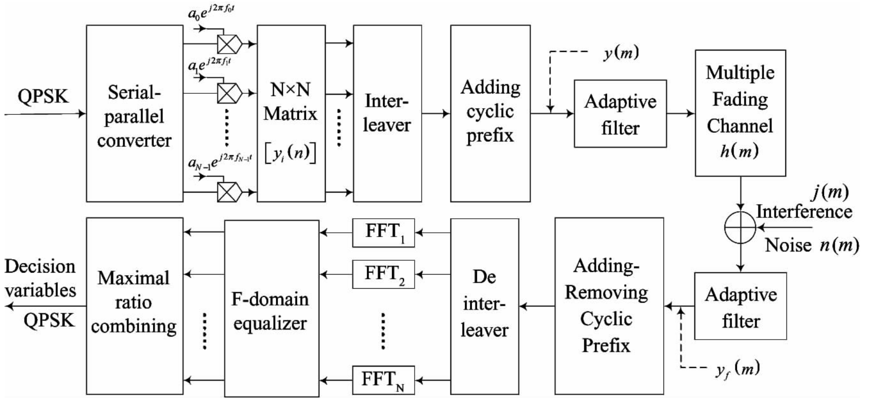

Fig. 1 Schematic diagram of system model

The generation of multiple subband signal is shown as follows[11-13]: $\alpha_i(i=0,1,\cdots,N)$ represents the ith complex symbol of N outgoing quadrature phase shift keying (QPSK) symbols, which will produce a multi subband OFDM signal after modulation and interleaving. $N\times 1$ parallel QPSK symbols from series-parallel conversion are modulated by corresponding N sub-carriers. If OFDM symbols cycle is T_s, $f_i = i/T_s$ represents the lth frequency of N orthogonal sub-carriers, and α_i will be modulated by the ith at t, where $t = nT_s/N$, $n=0,1,\cdots,N-1$. The modulated signal on the ith branch at the nth moment will be expressed as

$$y_i(n) = a_i e^{j2\pi f_i t} = a_i e^{j2\pi ni/N} \tag{1}$$

In an OFDM symbol cycle T_s, $N\times 1$ data symbol vectors are modulated by the same sub-carrier. So the input vectors will generate an $N\times N$ sample matrix after modulating. If the ith sub-carrier has been transferred first and τ is the interval, there will be $\tau = T_s/N^2$ and an OFDM symbol with N^2 samples will be formed by adding all sub-carriers after being transferred. The mth sample can be represented by $y(m)$, $m = nN+i$, $i = 0,1,\cdots,N^2-1$, as follows:

$$y(m) = \sum_i^N \sum_n^N y_i(n)\delta[m-i-nN] \tag{2}$$

where $\delta[m-i-nN]$ is the unit impulse as

$$\delta[m-i-nN] = \begin{cases}1, & m = nN+i\\ 0, & m \neq nN+i\end{cases} \tag{3}$$

$y(m)$ by interleaving only has nonzero value when there is $m = nN+i$, and in this case, $y(m)$ can be represented as

$$y(m) = y(nN+i) = y_i(n) \tag{4}$$

where $m = nN+i$ and n, $i = 0,1,\cdots,N-1$.

Frequency domain form of multiple subband OFDM signals could be obtained by time domain signal $y(m)$ being fast Fourier transformed as shown in Eq. (5).

$$\begin{aligned} Y(k) &= FFT[y(m)] = N\sum_{i=0}^{N-1} a_i e^{-j\frac{2\pi}{N^2}ki}\delta((k-i)_N) \\ &= N\sum_{i=0}^{N-1} a_i e^{-j\frac{2\pi}{N^2}ki}\frac{1}{N}\sum_{n=0}^{N-1} e^{-j\frac{2\pi}{N^2}(k-i)n} \end{aligned} \tag{5}$$

where i, $p = 0,1,\cdots,N-1$.

From all above, OFDM symbols are composed of N subbands and each data symbol α_i has been modulated to every kth sub-carrier, which can be called multiple subband signal of interleaving spread spectrum OFDM. The signal outline in N frequency subbands condition can be shown in Fig. 2.

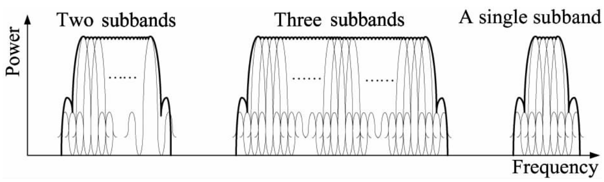

Fig. 2 Sketch map of N subbands ISS-OFDM outline

When the signal is transmitted in multipath fading channel, impulse delay replica caused by the reflection and scattering will produce unexpected interference. Assuming $h(m)$ is the unit impulse response to multipath fading channel and $y(m)$ is the corresponding transmitting signal, the received equivalent low-pass signal can be regarded as the sum of convolution of $h(m)$ and $y(m)$, the noise and the interference $j(m)$ will be shown as

$$r(m) = h(m) \otimes y(m) + n(m) + j(m) \quad (6)$$

where $n(m)$ represents the unexpected white complex Gaussian noise.

Effect of interference detection from the receiver is to demodulate parts of ISS-OFDM multiple subbands through parallel FFT, and to compensate channel distortion by frequency-domain equalization and maximal ratio combining, so as to obtain a series of decision variables V_k. Here whether the signal being interfered through the subbands of receiving filter will be suppressed, eliminated or not depends on the degree of impact on the transmitting signal.

2 Receiver adaptive filtering

The purpose of receiver adaptive filtering proposed in this paper is to change the pass band dynamically to make it approach to the available subbands of ISS-OFDM as closely as possible, and to greatly suppress the interference without any information loss based on predetermined threshold.

2.1 Impulse response to receiver filtering

The cosine roll-offs function model[14,15] has been adopted according to the characteristics of wireless mobile multi-hop communication network. The unit impulse response can be shown as

$$p(m) = \frac{\sin\left[\pi \frac{m}{T_c}(1-\beta)\right] + 4\beta \frac{m}{T_c}\cos\left[\pi \frac{m}{T_c}(1+\beta)\right]}{\pi \frac{n}{T_c}\left[1-\left(4\beta \frac{m}{T_c}\right)^2\right]} \quad (7)$$

where T_c is the sampling cycle, m is the time variable and β is the rolloff-factor[16-18] which takes 0.22 in this paper.

Different settings of sampling cycle T_c and filter order will obtain different filter impulse responses to match different numbers of frequency subbands. A form of adaptive filter impulse response can be seen in Fig. 3(a), the frequency domain response to which can be obtained by discrete Fourier transmission, as shown in Fig. 3(b).

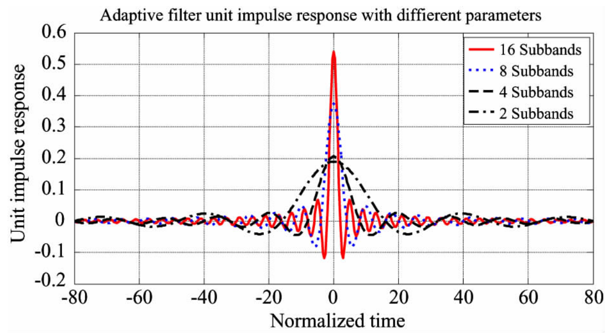

(a) Passbands with different numbers of subbands

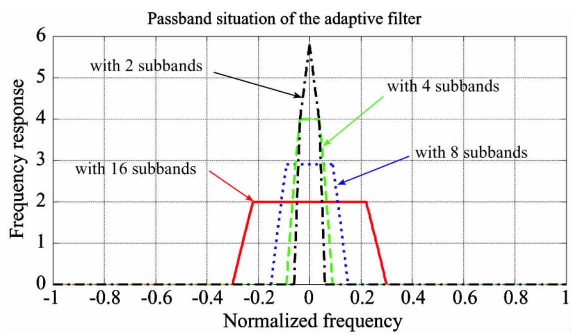

(b) Passbands with different numbers of subbands

Fig. 3 Filter characteristic response curves with different parameters

2.2 Receiver multiple subbands signal filtering

The process of multiple subbands signals passing the adaptive filter can be regarded as the convolution of the received signal and filter impulse response. The output signal of filter is shown as

$$y_f(m) = r(m) \otimes p(m) \quad (8)$$

where $y_f(m)$ represents the signal after filtering, and $p(m)$ is the filter unit impulse response.

If the bandwidth of the adaptive filter is designed to be equal to that of N subbands, the signal in the filtered passband will include N frequency subbands and each one will carry the entire original signal transmitting information. If the bandwidth M of the designed filter and number of sub-carriers N satisfy the relation of $M \leqslant N$, the only M subbands may pass the filter, that is to say, only M frequency subbands can be received and the transmitting information will be recovered by these M subbands. In the extreme case that the filter passband equals to single transmitting subband, this system model will degenerate to the traditional OFDM system.

The interference will exert an unexpected influence if the superposition on some subband reaches threshold γ_0, and all the interfered subbands will be filtered out. All the subbands will be allowed to pass with the interference lower than threshold γ_0, which means such kind of interference will hardly produce any serious result. Fig. 4 shows the process of 8 subbands passing the adaptive filter.

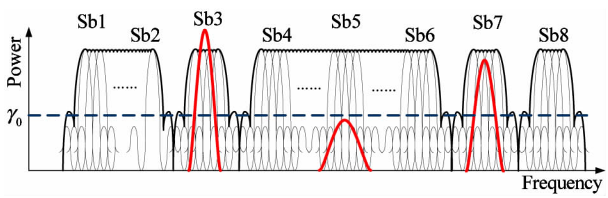

(a) Subbands of signal before adaptive filtering

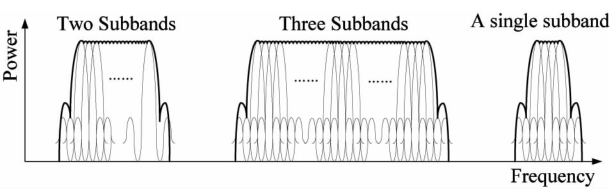

(b) Subbands of signal after adaptive filtering

Fig. 4 Filtering process of signal with 8 subbands

From Fig. 4(a) and Fig. 4(b), it can be seen that the 3rd and 7th subbands have been filtered out since the interference power past threshold γ_0, and the 5th subband has remained because of its low interference. In such case, the adaptive filter passband could be set to the bandwidth of the 2nd, 3rd or a single subband of the transmitting signal respectively, which will obtain a bandwidth of two, three, a single subband or their combinations after filter. Transmitting signal with different numbers of subbands will match flexibly to fill the spectral void.

3 Setting of determined threshold

The discussion above takes γ_0 as the known condition, and we will study how to obtain this threshold.

3.1 Determined threshold in Gaussian channel

Suppose M signals in those of N received frequency subbands are used for demodulation by a filter, and the power of each subband signal is P_S. If the power spectral density of the noise is N_0, the general power of interference signal on effective frequency band is P_J, and the bandwidth is B_J, which are distributed on l of M transmitting OFDM signal subbands. So power of all M subbands is MP_S, and signal-to-interference and noise (SINR) can be obtained by Eq. (9).

$$SINR_M = \frac{M \cdot P_S}{N_0 M \cdot B + P_J} = \frac{SNR}{1 + INR} \tag{9}$$

where $SNR = P_S / N_0 B$, $INR = P_J / N_0 MB$ represents interference- to-noise, and B is the bandwidth of a single subband.

If the processing gain of a single subband is G_p, $SINR^1_{Total}$ is the sum of $SINR_M$ of all M subbands as shown in Eq. (10).

$$SINR^1_{Total} = M \cdot G_p \cdot SINR_M = \frac{M \cdot G_p \cdot SNR}{1 + INR} \tag{10}$$

Similar to the derivation of $SINR_M$, if the interfered subband has been filtered out, the corresponding interfering power P_J will also be removed completely. Then $SINR$ through the adaptive filter will be transformed to Eq. (11).

$$SINR_{M-l} = \frac{(M-l) \cdot P_S}{N_0 (M-l) \cdot B} = SNR \tag{11}$$

From Eq. (10) we can see that after filtering out l interfered frequency subbands as well as considering the processing gain of a single subband, the total $SINR^2_{Total}$ of M-l subbands will be obtained by Eq. (12).

$$\begin{aligned} SINR^2_{Total} &= (M-l) \cdot G_p \cdot SINR_{M-l} \\ &= (M-l) \cdot G_p \cdot SNR \end{aligned} \tag{12}$$

Since the signal energy it distributed on the whole frequency band and in the meantime the interfered l subbands is filtered, the signal distributed on this l subbands will be filtered out as well, which will inevitably cause partial loss in signal energy. Hence, it is a significant step to filter it out selectively from all l frequency subbands in a reasonable way to realize interference suppression and not to destroy the signal reconstruction at the same time. We make the compromise available by calculating the interference threshold adaptively to direct the filtering dynamically in this paper. In a Gaussian channel, the performance of BER depends on the normal SNR or SINR. The bigger SINR will perform better. So the interference threshold could be obtained by adjusting $SINR^1_{Total}$ and $SINR^2_{Total}$ to satisfy Eq. (13).

$$SINR^2_{Total} > SINR^1_{Total} \tag{13}$$

To substitute $SINR^1_{Total}$ in Eq. (10) and $SINR^2_{Total}$ in Eq. (12) into Eq. (13), there is

$$INR > \frac{l}{M-l} = \gamma_0 \tag{14}$$

where γ_0 is the interference threshold.

From Eq. (14) it can be seen that INR threshold γ_0 is related to M (number of transmitting frequency subbands) and l (number of interfered subbands in Gaussian channel). Given the number of interfered subbands l ($l = 1,2,4,8$), INR threshold will decrease with the increase of the number of M. And if given the number of transmitting subbands M, INR threshold will increase with the increase of the number of interfered subbands l.

3.2 Determined threshold in multi-fading channel

The randomness of fading in a multipath fading channel will result in constant threshold in Gaussian channel not available. The system BER statistical performance in a multipath fading channel has been analyzed in this paper so as to obtain an estimation of the threshold. Based on Eq. (10) and considering the impact of multi-fading, BER could be expressed by Eq. (15) before being filtered out from interfered frequency subbands with the irrelevant part substituted by function Q.

$$P_e^1 = E_C\left[Q\left(\sqrt{\sum_{p=0}^{M-1} |H_p|^2 SINR_{Total}^1}\right)\right] = E_C\left[Q\left(\sqrt{\sum_{p=0}^{M-1} |H_p|^2 \frac{SNR}{1+INR}}\right)\right] \quad (15)$$

where $E_C(\cdot)$ is the statistical expectation of conditional error probability in a multiple fading channel, and the summation item of $|H_p|^2$ is the sum of M multiple fading channel parameters on M sub-carriers. Since QPSK has been adopted, there will be $SNR = (2/M)E_b/N_0$ where E_b/N_0 is the ratio of signal bit energy to noise spectrum density. Therefore, Eq. (15) will be re-represented to Eq. (16).

$$P_e^1 = E_C\left[Q\left(\frac{1}{M}\sqrt{\sum_{p=0}^{M-1} |H_p|^2 \frac{2\cdot E_b/N_0}{1+INR}}\right)\right] \quad (16)$$

Similarly, the system BER can be obtained by Eq. (17) after being filtered out from interfered subbands, where the parameters share the same definition as in Eq. (16).

$$P_e^2 = E_C\left[Q\left(\sqrt{\frac{1}{M}\sum_{p=0}^{M-l-1} |H_p|^2 \frac{2E_b}{N_0}}\right)\right] \quad (17)$$

The system BER performance changing with INR on 16 transmitting frequency subbands with $E_b/N_0 = 10$dB in the multiple fading channel has been simulated based on NS2[19,20] in this paper. The simulating result in Fig. 5 indicates that the system BER performance in the multipath fading channel shows a flat trend, when the interfered subbands ($l = 1,2,4,8$) with the same E_b/N_0 are filtered out. The intersection points of BER curves in Fig. 5 correspond to interference threshold of $l = 1,2,4$ and 8 respectively, and that are −11dB, −7.5dB, −4.0dB and 1dB.

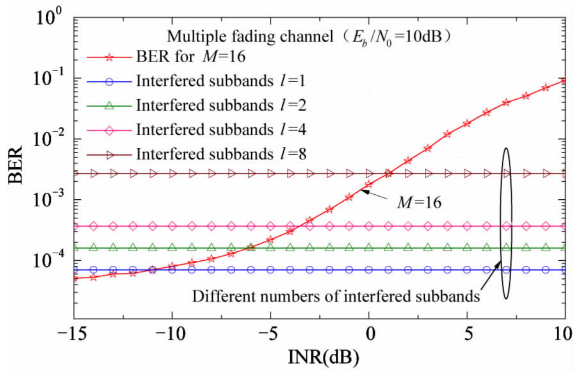

Fig. 5 INR threshold in multipath fading channels

The corresponding thresholds in Gaussian channels can be obtained by Eq. (15). Comparisons of results in these two channels with the number of transmitting subbands as $M = 2,4,8,16,32$ have been presented in Table 1. From this table we can see that the difference between the multipath fading channel and Gaussian channel decreases with the increase of the number of transmitting subbands and approaches to zero when there is $M = 32$. That is to say, the threshold in Gaussian channel can be taken to replace that in the multipath fading channel with the same condition when the transmitting subbands adopted are more than 32.

Table 1 Comparisons of thresholds (dB) in Gaussian channel and the multipath fading channel with $E_b/N_0 = 10$dB (G-Gaussian; M-Multiple Fading)

Interfered Subbands	$M = 2$		$M = 4$		$M = 8$		$M = 16$		$M = 32$	
	G	M	G	M	G	M	G	M	G	M
$l = 1$	0	4.9	−4.8	−1.7	−8.5	−5.5	−11.8	−11.0	−14.9	−14.5
$l = 2$	–	–	0	3.3	−4.8	−2.0	−8.5	−7.5	−11.8	−11.5
$l = 4$	–	–	–	–	0	3.0	−4.8	−4.0	−8.5	−8.5
$l = 8$	–	–	–	–	–	–	0	1.0	−4.8	−4.5
D-Value	≈4.9		≈3.2		≈3		≈1.0		≈0.3	

4 System performance analyses

The judgment will carried out based on the obtained INR threshold, and the interfered frequency subbands which exceed the threshold will be filtered out, or else be kept to extract the information. The system BER of a single interfered subband can be seen in Fig. 6 with $\gamma_0 = 3$dB when the number of transmitting subbands satisfies $M = 2, 4, 8, 16, 32$.

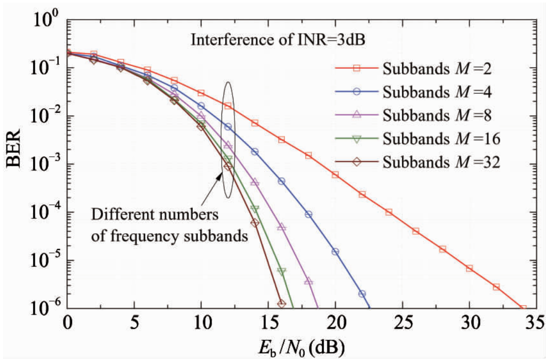

Fig. 6 BER figures of subbands with interference

And Fig. 7 shows the system BER performance after the interfered subbands are filtered out. It is not difficult to notice by comparing that the BER performance has improved by 0.5dB ~ 5dB after interference suppression when $M = 4, 8, 16, 32$. The system performance with $M = 2$, however, turns bad, which is because the signals are removed when the frequency subbands with interference threshold γ_0 lower than the filtering threshold $\gamma_0 = 4.9$dB are filtered out.

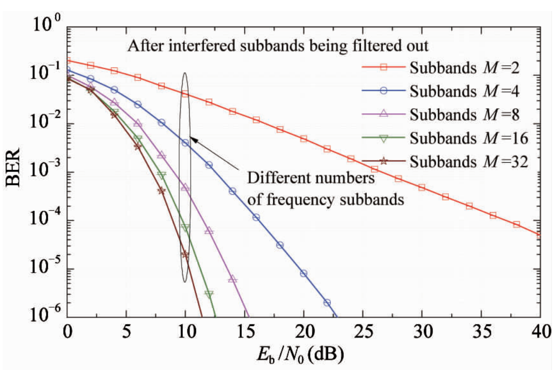

Fig. 7 BER figures of subbands without interference

These subbands may be selected randomly to match the spectrum gap without adopting a complex frequency hopping way based on the adaptive filtering game proposed in this paper. Moreover, some interfered subbands which are suppressed by the adaptive filtering will make ISS-OFDM signals turn to be series of subbands segments as shown in Fig. 4. These discrete frequency subbands can be demodulated and equalized respectively, then distributed on the corresponding sub-carriers of each subband. Such an approach can not only save the limited power, but also improve the spectrum utilization.

5 Conclusion

An ISS-OFDM based adaptive filtering mechanism with predetermined interference threshold has been proposed in this paper through adjusting the filter passband dynamically to match the corresponding effective frequency band for wireless multi-hop communication network. Such an adaptive approach takes full use of the transmitting subbands including parts of the interfered ones so as to save the signal power greatly. The random utilization of frequency subbands in a broad spectrum range is allowed without adopting the complex frequency hopping way. We have obtained the corresponding interference thresholds of Gaussian channel and the multipath fading channels by calculation-derivation and statistical method respectively in this paper. Simulating results based on NS2 show that the adaptive filtering mechanism and dynamic transmitting subbands selection algorithm have a positive significance to alleviate the limited spectrum and energy resources for wireless multi-hop communication network.

References

[1] Hwang R H, Wang C Y, Wu C J, et al. A novel efficient power-saving MAC protocol for multi-hop MANETs. *Int J Commun Syst*, 2013, 26(1): 34-55

[2] Zhu T, Zhong Z G, He T, et al. Achieving efficient flooding by utilizing link correlation in wireless sensor networks. *IEEE/ACM Trans Networking*, 2013, 21(1): 121-134

[3] Van N M, Lee S W, Hong C S. Joint rate adaption, power control, and spectrum allocation in OFDMA-based multi-hop CRNs. *IEICE Trans Commun*, 2013, E96-B: 242-253

[4] Basel A, Wail M, Hussein M. A Kalman-fuzzy application for rate adaptation in IEEE 802. 11 based multihop ad hoc networks. In: Proceedings of the 2011 International Conference on Wireless Communication Mobile Computing, Istanbul, Turkey, 2011. 243-248

[5] Yang X J, Xing K Y. Channel fault tolerant target tracking in multi-hop wireless sensor networks based on particle filtering. *Acta Auto Sin*, 2011, 37(4): 440-448

[6] Chen J, Ma T, Chen W J, et al. Unsupervised robust recursive least-squares algorithm for impulsive noise filtering. *Sci China Inf Sci*, 2013, 56(4): 1-10

[7] Zhao C L, Zhang K, Sun X B, et al. Precoding with interference suppression sequence scheme for OFDM-based

cognitive radio systems. *J China Univ Post Telecom*, 2011, 18(4): 59-64

[8] Feng D Q, Jiang C Z, Lim G B, et al. A survey of energy-efficient wireless communications. *IEEE Commun Surv Tutor*, 2013, 15(1): 167-178

[9] Aruna T, Suganthi M. Variable power adaptive MIMO OFDM system under imperfect CSI for mobile ad hoc networks. *Telecommun Syst*, 2012, 50(1): 47-53

[10] Senthil B, Aravind R, Prabhu K M M. Interleaving-based cyclic delay diversity OFDM systems over spatially correlated channels. *Circ Syst Signal Process*, 2013, 32(1): 283-297

[11] Huang Y C, Rao B D. Performance analysis of heterogeneous feedback design in an OFDMA downlink with partial and imperfect feedback. *IEEE Trans Signal Process*, 2013, 61(4): 1033-1046

[12] Shen G X, Cai A L, Peng L M. Benefits of sub-band virtual concatenation in co-OFDM optical networks. In: Proceedings of International Conference on Transparent Optical Networks, Coventry, UK, 2012. 1-4

[13] Yin W S, Ren P Y, Du Q H, et al. Delay and throughput oriented continuous spectrum sensing schemes in cognitive radio networks. *IEEE Trans Wireless Commun*, 2012, 11(6): 2148-2159

[14] Zandi M, Grami A. A new class of nyquist pulses with a monomial roll-off. In: Proceedings of Canadian Conference on Electrical Computer Engineering, Vancouver, Canada, 2011. 63-65

[15] Azurdia M C, Lee K J, Lee K S. ISI-free linear combination pulses with better performance. *IEICE Trans Commun*, 2013. E96-B(2): 635-638

[16] Mukherjee B, Samariya A L, Tiwari S. Improvement in roll off factor of low pass filter placed on an EBG substrate. *Frequenz*, 2013, 67(3): 73-78

[17] Yang H C, Wang M C. Evaluation of the capacitances by using high frequency roll-off fitting to the second order approximation. *Adv Mater Res*, 2011, 204: 554-557

[18] Tsai H F, Jiang Z H. Raised cosine interpolator filter for digital magnetic recording channel. *Eurasip J Adv Sign Process*, 2012, 20(7): 1205-1217

[19] Berkeley U. The Network Simulator ns-2. Part of the VINT Project. Available from http://www.isi.edu/nsna. 1998

[20] Zhang S F, Li S, Zhang X, et al. Topology building for multi-hop wireless networks based on 802.11Ext physical layer in NS2. In: Proceedings of International Conference on Computer Science and Service System, Nanjing, China, 2012. 773-776

Qin Danyang, born in 1983. She received her B. S. degree in communication engineering from Harbin Institute of Technology in 2006, and both M. S and Ph. D. degree in information and communication system from Harbin Institute of Technology in 2008 and 2011 respectively. Currently, she is a lecturer at the Department of Communication Engineering of Heilongjiang University, Harbin, P. R. China. Her researches include wireless sensor network, wireless multihop routing and ubiquitous sensing.